

SANDIA 0699C

RECEIVED
MAR 15 1996
OSTI

Optimized Input Shaping for a Single Flexible Robot Link

David G. Wilson[†], Dennis Stokes[†], Gregory Starr[†], and Rush D. Robinett[§]

Abstract

This paper will discuss the design of an input shaped open-loop control for a single flexible robot link. The authors develop the equations of motion, including the first flexible mode shape and the actuator dynamics. Additional content includes the hardware system identification iterative runs used to update the model. Optimized input shaped commands for the flexible robot link to produce a rest-to-rest, residual vibration-free, 90 degree maneuver are developed. Correlation between both experimental and analytical results of the 90° slew, using two different identification models, are reviewed.

Introduction

For Space applications, lightweight robotic manipulators are necessary to reduce launch costs, power consumption, and storage volume of the robot. Space Station assembly, operations, and satellite maintenance present a serious challenge to autonomous space-based robotics. To avoid large dangerous vibrations, the current Space Shuttle robotic arm must operate very slowly. The operator must wait more than a minute to allow the robotic arm to settle after a move. The engineers will achieve a decrease in the operation cost by minimizing the idle time during operation of the robotic arm (Singer89). Future Space applications will require lightweight robotic arms capable of accurately positioning larger payloads, performing tasks at high bandwidths, and exerting large external forces. All these applications increase structural bending of the members. One way to reduce the vibration is to generate optimized command trajectories that minimize the excitation of structural resonance. The objective of this paper is to design an input shaped command for a single flexible robot link to produce a rest-to-rest, residual vibration-free maneuver. The methodology includes development of the dynamic system equations of

[†] UNM Graduate Student, M.E. Dept., UNM, Albuquerque, NM 87131

[‡] UNM Professor, M.E. Dept., UNM, Albuquerque, NM 87131

[§] Sandia National Laboratories, Albuquerque, NM 87185

This work was supported by the
United States Department of Energy
under Contract DE-AC04-94AL85000.

motion; system identification; optimized trajectory design; and verification using the University of New Mexico's (UNM) single flexible robot link hardware testbed.

Dynamic Equations of Motion

The dynamic equations of motion were developed for a unidirectional rotating beam using quadratic modes (Segalman90) and with consideration of a tip mass. Figure 1 shows a schematic of the flexible robot link defining the mathematical geometry along with a table of the physical parameters.

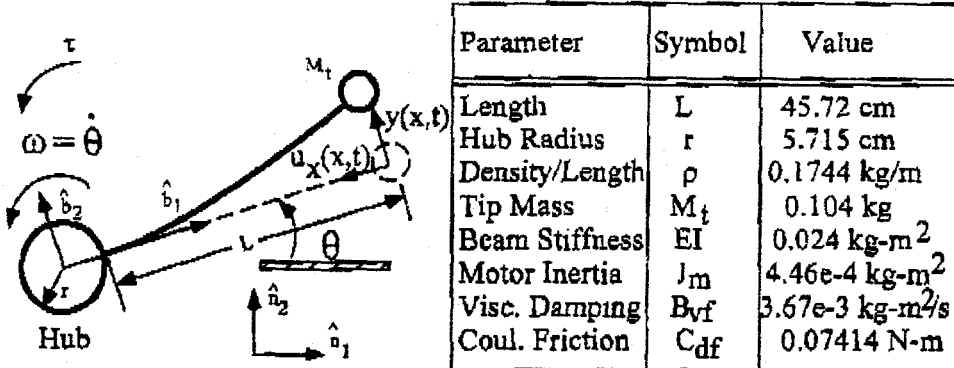


Figure 1: Flexible Beam Schematic and Physical Parameters

An expression for the deformation of a point along the beam is

$$u(x, t) = u_x(x, t)\hat{b}_1 + y(x, t)\hat{b}_2.$$

Define the following relationships for axial and transverse deflections as

$$u_x(x, t) = -\frac{1}{2} \int_0^x \left(\frac{dy(\xi, t)}{d\xi} \right)^2 d\xi$$

and

$$y(x, t) = \sum_{i=1}^{\infty} \phi_i(x) q_i(t).$$

The transverse deflection is composed of $\phi_i(x)$, the mode shape basis functions and $q_i(t)$, the corresponding time-dependent generalized coordinates. The following equation gives the velocity of each point along the rotating beam's length:

$$\nu(x, t) = \frac{N}{dt} \left\{ [r + x]\hat{b}_1 + u(x, t) \right\}.$$

The kinetic energy, T , of the beam is

$$T = \frac{1}{2} \int_0^L \bar{\rho} \nu(x, t) \cdot \nu(x, t) dx,$$

where $\bar{\rho} = \rho + M_i \delta(x - L)$. The strain energy, U , is

$$U = \frac{1}{2} \int_0^L EI \left(\frac{\partial^2 y(x, t)}{\partial x^2} \right) dx,$$

and the generalized work term as $W = \tau d\theta$. Performing the mathematical expansions and substituting the expressions for the work, kinetic, and strain energies into Lagrange's equations, we obtain the following equations for beam deflection and rotation, respectively.

$$\left\{ EI \int_0^L \phi_i'' \phi_j'' dx - \left(\bar{\rho} \int_0^L \phi_i \phi_j dx + 2\bar{\rho} \int_0^L [r + x] g_{ij} dx \right) \omega^2 \right\} q_i \quad (1)$$

$$+ \left[\bar{\rho} \int_0^L \phi_i \phi_j dx \right] \ddot{q}_i = - \left[\bar{\rho} \int_0^L [r + x] \phi_i dx \right] \dot{\omega}$$

$$\left[\frac{1}{3} \rho L^3 + \rho r L^2 + \rho r^2 L + M_i (r + L)^2 \right] \ddot{\theta} + \left[\bar{\rho} \int_0^L x \phi_i dx \right] \ddot{q}_i = \tau \quad (2)$$

For mode 1, a static force basis of $\phi_1(x) = 3Lx^2 - x^3$, was selected and the quadratic modes for a beam were defined as $g_{ij} = -\frac{1}{2} \int_0^x \phi_i'(\xi) \phi_j'(\xi) d\xi$.

The actuator dynamics are $\tau = J_m \ddot{\theta} + b_{v,f} \dot{\theta} + c_d \text{sign}(\dot{\theta})$. This model includes both a viscous friction and a Coulomb friction term. The inertia is the rotational inertia seen at the hub. A PD control law is used to drive the motor; $\tau = K_p(\theta_c - \theta) - K_d \dot{\theta}$, where K_p and K_d are the position and derivative gains, respectively, and θ_c is the commanded input.

Combining the equations for the beam deflection (1), beam rotation (2), actuator dynamics, and control law results in the following matrix equation;

$$M\ddot{x} + C\dot{x} + [J^2 K_c + K]x = Bu, \quad (3)$$

where $x = \{\theta \ q_1\}^T$, $B = \{K_p \ 0\}^T$, $u = \theta_c$ and in (Wilson95) are the remaining matrix definitions.

System Identification

We fit models using a 90° step-input command to drive the motor and hub assembly and flexible beam. The initial model was a simple second-order system. Tuning natural frequency and damping ratio to $\omega_n = 4.147 \text{ rad/sec}$ and $\zeta = 0.145$ achieved an approximate fit to the simple second-order system. Equation (3), which defines a "high fidelity" model of the system was used for the second model. Most of the model coefficients were found to a high confidence level, except the Coulomb friction term. To obtain a good estimate of the Coulomb friction term, we tuned the high fidelity model, using the first modal frequency from the second-order model. Figure 2 shows step responses of both models along with the experimental response.

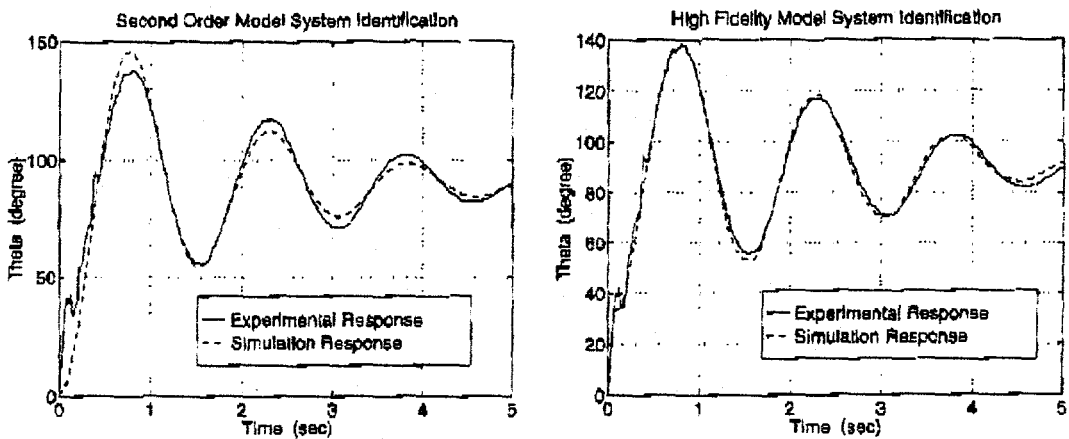


Figure 2: Model Identification Calibration Plots

Optimized Input Shaped Trajectory

We formulated a constrained optimization problem for the single flexible link using both the second-order model and the high fidelity model. Solving the trajectory optimization problem required the use of a Recursive Quadratic Programming (RQP) algorithm, VF02AD (Hopper78). The problem used 20 discretized temporal control inputs as parameters. The second-order model used the following performance index: $\phi(\xi) = 5(\dot{\theta}(t_f))^2$, with the following constraints: $\psi_1(\xi) = \theta(t_f) - \frac{\pi}{2}$ and $\psi_2(\xi) = \theta_c(t_f) - \frac{\pi}{2}$. The definition of a third state sets the controlled variable to the commanded input rate; $u = \dot{\theta}_c$.

To determine a starting point, the high fidelity model formulation used the following performance index: $\phi(\xi) = \int_0^{t_f} [\dot{\theta}(t)^2 + q(t)^2 + \dot{q}(t)^2] dt$, with the following constraints: $\psi_1(\xi) = \theta(t_f) - \frac{\pi}{2}$ and $\psi_2(\xi) = \theta_c(t_f) - \frac{\pi}{2}$, which approximately converged. This initial run helped put the parameters into the neighborhood of an optimal trajectory. The results of the previous run led to new parameter values, and the performance index reconfigured to the following: $\phi(\xi) = 0.5 \int_0^{t_f} u^2 dt + 20(\dot{\theta}(t_f))^2$, with the following constraints: $\psi_1(\xi) = \theta(t_f) - \frac{\pi}{2}$, $\psi_2(\xi) = q(t_f) - 0.0$, $\psi_3(\xi) = \dot{q}(t_f) - 0.0$, and $\psi_4(\xi) = \theta_c(t_f) - \frac{\pi}{2}$. The control variable remained the same, e.g., $u = \dot{\theta}_c$.

Experimental / Predicted Results

The UNM flexible testbed consists of a flexible aluminum link, the dimensions of which are 45.72 cm x 7.62 cm x 0.8128 mm; motor/hub/link mounting hardware; an electric DC servo motor; an incremental encoder; and a VME real-time control computer. The trajectories used as command inputs to the servo system, at 50 Hz sampling, were the result of the optimization procedure. Included in this report are two different runs. The first run used the optimized trajectory found with the second order model, while the second run used that found with the high fidelity model. Both runs are for a final time of $t_f = 2.0$ seconds. Figure 3 shows each run and contains the plots of the shaped input; experimental and simulated responses. The improved results of

the high fidelity run illustrates the effect of nonlinear friction compensation.

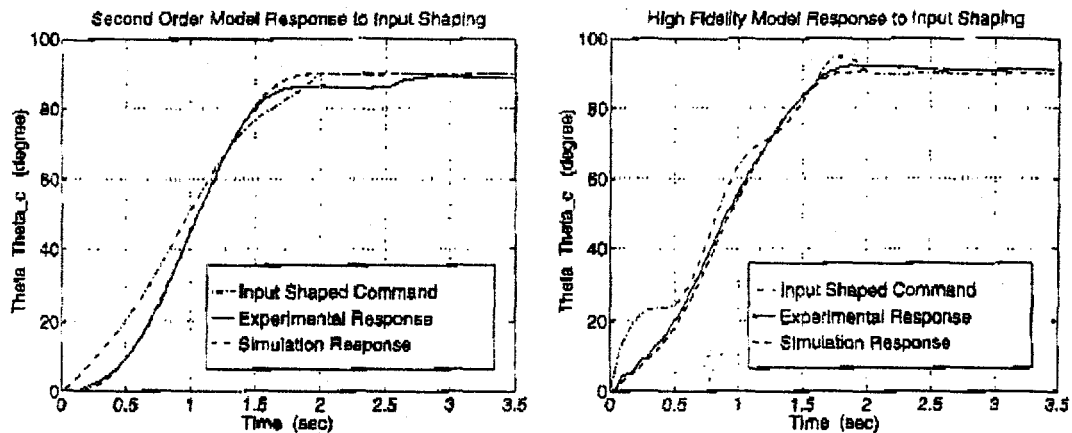


Figure 3: Optimized Input Arm Responses for Each Run

Conclusions

The authors successfully designed several optimized input shaped trajectories to minimize vibration during motion. Initially, an optimized trajectory with specific end-conditions was designed using a simple second-order model, using the experimental step response. Presence of unmodeled Coulomb friction produced inaccuracy between the predicted and experimental responses. The development of a high fidelity model, including dynamics of the flexible link, the motor, and nonlinear friction, allowed the optimization procedure to form trajectories which were a better match to the hardware. The optimized trajectories were tested experimentally and showed good correlation with the predicted responses, with minimal residual vibration.

References

- (Hopper78) Hopper, M.J., Harwell Subroutine Library, AERE-R9185, UKAEA, Harwell, Oxon, UK, 1978.
- (Segalman90) Segalman, D.J., Dohrmann, C.R., *Dynamics of Rotating Flexible Structures by a Method of Quadratic Modes*, Sandia National Laboratories, SAND90-2737, December 1990.
- (Singer89) Singer, Neil C., *Residual Vibration Reduction in Computer Controlled Machines*, MIT Artificial Intelligence Laboratory, Technical Report 1030, February 1989.
- (Wilson95) Wilson, David G., Stokes, Dennis, *Optimized Input Shaping and Control for a Single Flexible Robot Arm*, Final Project, UNM, ME Department, May 1995.

DISCLAIMER

This report was prepared as an account of work sponsored by an agency of the United States Government. Neither the United States Government nor any agency thereof, nor any of their employees, makes any warranty, express or implied, or assumes any legal liability or responsibility for the accuracy, completeness, or usefulness of any information, apparatus, product, or process disclosed, or represents that its use would not infringe privately owned rights. Reference herein to any specific commercial product, process, or service by trade name, trademark, manufacturer, or otherwise does not necessarily constitute or imply its endorsement, recommendation, or favoring by the United States Government or any agency thereof. The views and opinions of authors expressed herein do not necessarily state or reflect those of the United States Government or any agency thereof.